NONLINEAR ANALYSIS OF AN AXISYMMETRIC STRUCTURE SUBJECTED TO NON-AXISYMMETRIC LOADINGS

P.C. Chen and R.L. McKnight
General Electric Company
Cincinnati, Ohio 45215

The development of the SHELPC finite element computer program is detailed. This program is specialized to simulate the nonlinear material behavior which results from combustor liner "hot streaks". This problem produces a nonlinear Fourier Series type loading on an axisymmetric structure. Example cases are presented.

One problem which is unique to Aircraft Gas Turbine Engines (AGTE's) is the thermal hot streak problem experienced by certain combustor liners. These liners are thin axisymmetric pressure shells whose function is to contain and promote the combustion process. Because of the high temperatures involved in this combustion process, the functioning of these liners depends on their being "cooled" by lower temperature air from the compressor. To complicate this problem further, the temperatures generated by the combustion process are not uniform in either the axial or circumferential directions of the combustor liner.

The temperature variation in the axial direction is the variation normally shown in textbooks and calculated from the thermodynamic laws based on pressure/volume considerations. The circumferential variation is a more complex, three dimensional mixing problem. It is a function of the number of fuel nozzles employed and the geometry and thermodynamics of the combustor. The result is a circumferential variation in the metal temperature of these liners which can be approximated with Fourier Series.

The functional lives of these liners are primarily dictated by the resulting material response to these temperature variations, which produce thermal stresses. The stresses produced by the differential pressures across the liner walls are limited to small values and are secondary contributors to the problem. Because of the high temperatures and large temperature variations involved, the material response problem is nonlinear and time dependent. AEBG has been active in developing internal computer tools for attacking these types of unique AGTE problems. Our capabilities include both two-dimensional and three-dimensional nonlinear finite element computer programs.

The thermal stress problem generated by the axial variation in metal temperatures can be handled quite readily by a two-dimensional (axisymmetric) analysis. However, the thermal stresses generated by the circumferential variation in metal temperatures is truly a three-dimensional problem. As such, one method of attack would be to develop a simulation using three-dimensional finite elements, such as our 8, 16 or 20 noded isoparametric elements.

This method of attack has drawbacks in economy, accuracy, and utility. The number of hot streaks can be quite large (in the 60's) and the hot to cold temperature variations can be in the hundreds of degrees Fahrenheit. This would require a large number of 3D elements to produce an acceptable simulation. This could also produce bad element aspect ratios, resulting in solution accuracy problems. Varying these models in an iterative design process would be manpower and computer intensive. For these reasons we sought other methods of attacking this problem.

Since the circumferential temperature variations can be represented as Fourier Series expansions, this suggests attacking the structural problem by means of Fourier Series. This method of attack for linear elastic problems in a finite element format was presented by E.L. Wilson in Reference (1). For linear elastic problems the method of superposition of Fourier Series loading is mathematically exact and precise. However the problem in question is nonlinear.

In Reference (2), E.A. Witmer and J.J. Kotanchik presented a nonlinear solution procedure for axisymmetric shells under asymmetrical loading. In their approach, they utilized an initial strain method with Besseling's isothermal constitutive model in a sublayer format. This then presented a method of attacking nonlinear Fourier Series loading problems but with one tremendous deficiency; our problem under consideration is totally nonisothermal in nature.

Subsequently, one of the present authors, R.L. McKnight, developed a variable temperature version of Besseling's constitutive model in a subvolume format as presented in References (3) and (4). This has been the primary basis of AEBG's internal nonlinear computer tools since 1975. To this time-independent plasticity formulation, we added classical creep capability with time-hardening, strain-hardening, and life-fraction rules for attacking quasi-static time-dependent nonlinear problems. Over the years, through large amounts of production usage, these tools have been provided with much verification, validation, and operational experience for both 2D and 3D problems. With this background, we decided to reattack the combustor liner hot streak problem:

SHELPC

The following is a synopsis of the theoretical development of the combustor liner program, SHELPC. A complete development will be found in the Ph.D. Dissertation of P.C. Chen, to be published later.

As in Reference (1), the finite element employed is the triangular ring element shown in Figure 1. This is an extension of that element commonly used for plane stress, plane strain, and axisymmetric analysis. In those cases, there are two degrees of freedom, or displacements at each node. To allow for

the circumferential variation in load a third degree of freedom, the circumferential or hoop displacement, is introduced. These three displacement components are assumed to be linear functions of position in the R-Z plane. This is expressed mathematically as follows

$$\begin{aligned} U_R &= b_1 + b_2R + b_3Z \\ U_Z &= b_4 + b_5R + b_6Z \\ U_S &= b_7 + b_8R + b_9Z \end{aligned} \tag{1}$$

The strain components in terms of these displacements are (for small displacement theory).

$$\begin{aligned} \varepsilon_R &= \frac{\partial U_R}{\partial R} \\ \varepsilon_Z &= \frac{\partial U_Z}{\partial Z} \\ \varepsilon_\theta &= \frac{1}{R}\frac{\partial U_\theta}{\partial \theta} + \frac{U_R}{R} \\ \varepsilon_{RZ} &= \frac{\partial U_R}{\partial Z} + \frac{\partial U_Z}{\partial R} \\ \varepsilon_{Z\theta} &= \frac{\partial U_\theta}{\partial Z} + \frac{1}{R}\frac{\partial U_Z}{\partial \theta} \\ \varepsilon_{\theta R} &= \frac{1}{R}\frac{\partial U_R}{\partial \theta} + \frac{\partial U_\theta}{\partial R} - \frac{U_\theta}{R} \end{aligned} \tag{2}$$

The loading is now allowed to varying in the circumferential direction in a sine or cosine fashion as defined in Table 1.

Equations (1), then become

$$\begin{aligned} U_R &= (b_{1n} + b_{2n}R + b_{3n}Z)\ \cos N\theta \\ U_Z &= (b_{4n} + b_{5n}R + b_{6n}Z)\ \cos N\theta \\ U_\theta &= (b_{7n} + b_{8n}R + b_{9n}Z)\ \text{Sin}\ N\theta \end{aligned} \tag{3}$$

or

$$\begin{aligned} U_R &= (b_{1n} + b_{2n}R + b_{3n}Z)\ \text{Sin}\ N\theta \\ U_Z &= (b_{4n} + b_{5n}R + b_{6n}Z)\ \text{Sin}\ N\theta \\ U_\theta &= (b_{7n} + b_{8n}R + b_{9n}Z)\ \text{Cos}\ N\theta \end{aligned} \tag{4}$$

TABLE 1

FOURIER SERIES LOADING AND DISPLACEMENT DESCRIPTION

Symmetric about a plane containing the axis of revolution	Anti-symmetric about a plane containing the axis of revolution
$T = \Sigma T_n(r,z) \cos n\theta$	$T = \Sigma T_n(r,z) \sin n\theta$
$S_r = \Sigma S_{rn}(r,z) \cos n\theta$	$S_r = \Sigma S_{rn}(r,z) \sin n\theta$
$S_z = \Sigma S_{zn}(r,z) \cos n\theta$	$S_z = \Sigma S_{zn}(r,z) \sin n\theta$
$S_\theta = \Sigma S_{\theta n}(r,z) \sin n\theta$	$S_\theta = \Sigma S_{\theta n}(r,z) \cos n\theta$
$U_r = \Sigma U_{rn}(r,z) \cos n\theta$	$U_r = \Sigma U_{rn}(r,z) \sin n\theta$
$U_z = \Sigma U_{zn}(r,z) \cos n\theta$	$U_z = \Sigma U_{zn}(r,z) \sin n\theta$
$U_\theta = \Sigma U_{\theta n}(r,z) \sin n\theta$	$U_t = \Sigma U_{tn}(r,z) \cos n\theta$

n is the harmonic number.

T is the temperature.

S's are the loads.

U's are the displacements.

To introduce nonlinear material behavior, we make the classical assumption that the total strains consist of a summation of elastic, plastic, creep, and thermal components

$$\varepsilon = \varepsilon^e + \varepsilon^P + \varepsilon^C + \varepsilon^T \tag{5}$$

We also assume that stress is linearly related to the elastic strain only

$$\sigma = C\,\varepsilon^e \tag{6}$$

$$\sigma = C(\varepsilon - \varepsilon^P - \varepsilon^C - \varepsilon^T) \tag{7}$$

Where C is the elastic Hook's Law matrix.

The sum of the plastic, creep, and thermal strains are considered as initial strains.

$$\varepsilon^I = \varepsilon P + \varepsilon C + \varepsilon T \tag{8}$$

or

$$\sigma = C(\varepsilon - \varepsilon^I) \tag{9}$$

Applying the precepts of Reference (2), we make use of the Principle of Stationary Total Potential Energy.

The strain energy density is expressed as

$$\bar{U} = \tfrac{1}{2}\,\sigma^T\,\varepsilon^e \tag{10}$$

or

$$\bar{U} = \tfrac{1}{2}[C(\varepsilon - \varepsilon^I)^T]\,(\varepsilon - \varepsilon^I) \tag{11}$$

$$\bar{U} = \tfrac{1}{2}\,(\varepsilon - \varepsilon^I)^T\,C(\varepsilon - \varepsilon^I) \tag{12}$$

The total potential energy of one ring element is

$$PE = \int_V \tfrac{1}{2}(\varepsilon - \varepsilon^I)^T\,C\,(\varepsilon - \varepsilon^I)dV - \delta^T F \tag{13}$$

where δ is the generalized displacements and F is the generalized external forces.

For a system of ring elements, this development leads to

$$K\delta = F + F^I \tag{14}$$

where

K = elastic stiffness matrix for discretized system

δ = generalized displacements of the discretized system

F = applied generalized forces

F^I = generalized forces due to initial strains

Now, to introduce the Fourier Series loading into this system of equations. Our assumption is that the total strain can be considered to be made up of the sum of a certain number of A-series and B-series Fourier components. The A-series components are those symmetrical about a plane containing the axis of rotation. The B-series components are those antisymmetrical about a plane containing the axis of rotation (see Table 1). Thus we assume

$$U(R,Z,\theta) = \Sigma\, U_N^A\,(R,Z)\cos N\theta + \Sigma\, U_N^B\,(R,Z)\,\mathrm{Sin}\,N\theta \tag{15}$$

and therefore

$$\varepsilon(R,Z,\theta) = \Sigma\, \varepsilon_N^A\,(R,Z)\cos N\theta + \Sigma\, \varepsilon_N^B\,(R,Z)\,\mathrm{Sin}\,N\theta \tag{16}$$

or

$$\varepsilon(R,Z,\theta) = \varepsilon^A(R,Z,\theta) + \varepsilon^B(R,Z,\theta) \tag{17}$$

and, using Equation (5)

$$\begin{aligned}\varepsilon(R,Z,\theta) = {} & \varepsilon^{eA}(R,Z,\theta) + \varepsilon^{PA}(R,Z,\theta) + \varepsilon^{CA}(R,Z,\theta) \\ & + \varepsilon^{TA}(R,Z,\theta) + \varepsilon^{eB}(R,Z,\theta) \\ & + \varepsilon^{PB}(R,Z,\theta) + \varepsilon^{CB}(R,Z,\theta) \\ & + \varepsilon^{TB}(R,Z,\theta)\end{aligned} \tag{18}$$

For a discretized model, the system of equations are set up and solved a harmonic and a series at a time

$$[K_N^A]\ \delta_N^A = F_N^A + F_N^{IA} \tag{19}$$

$$[K_N^B]\ {}^B_N = F_N^B + F_N^{IB} \tag{20}$$

The nodal displacements are then given by

$$\delta(R,Z,\theta) = \Sigma\, \delta_N^A \cos N\theta + \Sigma\, \delta_N^B \sin N\theta \tag{21}$$

NONLINEAR SOLUTION SCHEME

A given axisymmetric geometry with thermal and mechanical loadings which can be simulated by Fourier Series is first discretized by triangular rings. The pertinent system of equations, (19) and (20), are set up and solved, first assuming elastic behavior. This gives a first approximation for the nodal point displacements. With these results, which are the amplitudes of Fourier Series displacement components, we can now determine the displacements at any circumferential location.

A minimum period is selected based on the lowest order harmonic other than 0 (for the combustor liner this is determined by the number of fuel nozzles). This minimum period is then approximated by 10 points in the θ-direction. At each of these 10 points, each rings nodal point displacements can be determined. From this the total strain can be determined for each location. Then using the constitutive models as covered in References (3) and (4), an initial estimate is made for the inelastic strains and from these inelastic pseudo-forces, F^P and F^C. These inelastic pseudo-forces are then approximated by the Fourier Series harmonics.

$$\begin{aligned} F^P(R,Z,\theta) &= \Sigma F_N^{PA}(R,Z) \cos N\theta + \Sigma F_N^{PB}(R,Z) \sin N\theta \\ F^C(R,Z,\theta) &= \Sigma F_N^{CA}(R,Z) \cos N\theta + \Sigma F_N^{CB}(R,Z) \sin N\theta \end{aligned} \tag{22}$$

The amplitudes of these harmonic pseudo-forces are then added to the initial force vector.

$$\begin{aligned} F_N^I(R,Z,\theta) = {} & F_N^{TA}(R,Z) \cos N\theta + F_N^{TB}(R,Z) \sin N\theta \\ & + F_N^{PA}(R,Z) \cos N\theta + F_N^{PB}(R,Z) \sin N\theta \\ & + F_N^{CA}(R,Z) \cos N\theta + F_N^{CB}(R,Z) \sin N\theta \end{aligned} \tag{23}$$

This new value for the initial force vector is used to obtain a new series of solutions. From these, new inelastic strains are predicted and from these a third initial force vector. This process is continued until convergence occurs.

EXAMPLE CASES

In order to verify the correctness of the solution scheme as outlined, several comparisons with finite element methods were made. Two problems analyzed are presented, one representing combined thermoplasticity and creep under cyclic loading, and the other a verification of the elastic Fourier series analysis capability. These cases represent a check on the two basic aspects of the combined elastic/plastic technique for harmonic loading.

In the first case, which verifies the cyclic plasticity and creep capability, a thick-walled cylinder is subjected to a time-varying pressure and temperature loading history (Figure 2). These loadings are the predominant types experienced by combustors. Plane strain conditions were assumed, the finite element model being composed of triangular ring elements as shown in Figure 3. The model was also run using the CYANIDE 2-D computer code, subjected to the same temperature and pressure history as shown in Figure 2. The comparison between SHELPC and CYANIDE 2-D under these axisymmetric loadings was then made, the results being presented in Figures 2 and 4. Figure 2 shows a comparison of radial displacement versus time for the two methods. Figure 5 shows the residual stress distribution through the wall at t = 10 hours when the pressure was equal to zero. As can be seen from these results, correlation was very good.

A second test case was used to check the Fourier series method under a thermal loading represented by the combination of temperature harmonics of the form:

$$T(\theta) = 70 + 30 \cos(4\theta)$$

In an actual component, such as a combustor, the harmonics used would be a function of the number of "hot streaks" around the circumference. The model used was again a thick-walled cylinder as shown in Figure 3. To verify the response of the structure to this type of loading, the same model was run using the CLASS/MASS code which also has harmonic loading capability but limited to linear elastic behavior. This problem was run elastically with SHELPC in order to achieve a direct comparison. Results are presented in tabular form to demonstrate the closeness of the numerical comparison. In Table 2, the displacement components from SHELPC and CLASS/MASS are compared for the harmonic loading:

$$T(\theta) = 30 \cos(4\theta)$$

Table 2: Nodal Displacements at $\theta = 0^{o}$ Due to a Single Harmonic Thermal Load $T(\theta) = 30 \cos(4\theta)$.

Node No.	SHELPC (10^{-5} inch)			CLASS/MASS (10^{-5} inch)		
	δ_R	δ_Z	δ_θ	δ_R	δ_Z	δ_θ
1	-8.947	-7.726	8.633	-8.958	-7.736	8.641
2	-8.946	7.727	8.633	-8.958	7.736	8.641
3	-0.2380	0	3.661	-0.2445	0	3.646
4	7.718	-8.767	9.678	7.719	-8.770	9.678
5	7.718	8.767	9.678	7.719	8.770	9.678

In Table 3, the individual harmonic results from SHELPC for the displacements, stresses and strains are shown. The results from a combined harmonic run are also tabulated. As can be seen from this table, the results are correctly superimposed. They also correlate well with the corresponding CLASS/MASS values.

Table 3. Nodal Displacements and Element Strains and Stresses at $\theta = 0$ Due to Combined Harmonic Thermal Load (i.e., $T(\theta) = 70 + 30 \cos 4\theta$).

Nodal Displacements (10^{-3} Inch)

Node No.	n=0			n=4			Combined		
	δ_R	δ_Z	δ_θ	δ_R	δ_Z	δ_θ	δ_R	δ_Z	δ_θ
1	0.4200	-0.2100	0	-0.08947	-0.07726	0.08633	0.3305	-0.2873	0.08655
2	0.4200	0.2100	0	-0.08946	0.07727	0.08633	0.3305	0.2873	0.08633
3	0.6300	0	0	-0.02380	0	0.03661	0.6276	0	0.03661
4	0.8400	-0.2100	0	0.07718	-0.08767	0.09678	0.9172	-0.2977	0.09678
5	0.8400	0.2100	0	0.07718	0.08767	0.09678	0.9172	0.2977	0.09678

Element Strains (10^3 Inch/Inch)

Ele. No.	n=0				n=0				Combined			
	ε_r	ε_Z	ε_θ	$\varepsilon_{\theta r}$	ε_r	ε_Z	ε_θ	$\varepsilon_{\theta r}$	ε_r	ε_Z	ε_θ	$\varepsilon_{\theta r}$
1.	0.420	0.420	0.420	0	0.174	0.155	0.187	-0.0480	0.594	0.575	0.607	0.0480
2	0.420	0.420	0.420	0	0.167	0.165	0.192	-0.0253	0.557	0.585	0.612	0.0253
3	0.420	0.420	0.420	0	0.167	0.165	0.192	-0.0254	0.587	0.585	0.612	0.0254
4	0.420	0.420	0.420	0	0.157	0.175	0.195	-0.0320	0.579	0.595	0.615	-0.0320

Element Stresses (10^3 psi)

Ele. No.	n=0				n=0				Combined			
	σ_r	σ_Z	σ_θ	$\sigma_{\theta r}$	σ_r	σ_Z	σ_θ	$\sigma_{\theta r}$	σ_r	σ_Z	σ_θ	$\sigma_{\theta r}$
1	0	0	0	0	-0.549	-1.00	-0.244	0.553	-0.549	-1.00	-0.244	0.553
2	0	0	0	0	-2.592	-0.631	-0.005	-0.292	-0.592	-0.631	-0.005	-0.92
3	0	0	0	0	-0.591	-0.631	-0.005	-0.293	-0.591	-0.631	-0.005	-0.93
4	0	0	0	0	-0.664	-0.289	0.165	-0.370	-0.664	-0.289	-0.165	-0.370

Then three more complex nonlinear comparison cases were run to demonstrate the capabilities of SHELPC. These cases demonstrate elastic/plastic comparisons for axisymmetrically loaded structures as well as harmonic summation comparisons in the elastic regime. Since no other code which does the harmonic analysis was available, a direct comparison of nonlinear harmonic analysis could not be made. This comparison will rely primarily on experimental results from actual combustors.

To compare the elastic/plastic analysis capability for axisymmetric loading, we modeled a typical axisymmetric combustor lip, as shown in Figure 5. It was modeled using 168 3-node finite elements in both SHELPC and CYANIDE 2-D programs. The axisymmetric loading conditions were run and compared satisfactorily. Figures 6 and 7 show comparisons of the effective stress and effective plastic strain, respectively, as predicted by the two programs. The plot is for the inner surface of the cooling louver around the edge from element No. 56 to element No. 136 as shown in Figure 8. As can be seen from these results, the comparison between the two programs is excellent. This case was one of those used to validate the analytical development of SHELPC where a direct comparison with axisymmetric loads (zero harmonic) could be made.

Our second example demonstrates the Fourier series capability of SHELPC under a mechanical loading situation. Figure 9 gives the particulars of the problem, a ring under a harmonic pressure distribution applied at the outer diameter. This problem was solved both elastically and plastically for the stress-strain properties shown. Figure 10 shows the SHELPC predictions for the radial displacement at the outer diameter for the two cases. The elastic results were correlated with hand calculations and CLASS/MASS results.

As a final validation example, we extended the previous comparison with CLASS/MASS to the nonlinear regime.

Figure 11 shows the problem conditions, an increased thermal loading, and the assumed stress-strain curve. The elastic solution was correlated with CLASS/MASS. The plastic solution shows the difference in effect between the pressure load of the previous example and a thermal hot streak, Figure 12. In this case, plastic flow reduces the radial displacement.

This program is continuing under development with more verification and validation cases being pursued.

REFERENCES

1. Wilson, E. L., "Structural Analysis of Axisymmetric Solids," AIAA J., Vol. 3, No. 12, pp. 2269-2274, Dec. 1965.

2. Witmer, E. A. and Kotanchik, J. J., "Progress Report on Discrete-Element Elastic and Elastic-Plastic Analyses of Shells of Revolution Subjected to Axisymmetric and Asymmetric Loading," AFFDL-TR-68-150, pp. 1341-1453, Proceedings of the Second Conference on Matrix Methods in Structural Mechanics, WPAFB, Ohio, October 1968.

3. McKnight, R. L., "Finite Element Cyclic Thermoplasticity Analysis by the Method of Subvolumes," Ph.D. Dissertation, University of Cincinnati, 1975.

4. McKnight, R. L. and Sobel, L. H., "Finite Element Cyclic Thermoplasticity Analysis by the Method of Subvolumes," Compt. Structures, Vol. 7, No. 3, 1977.

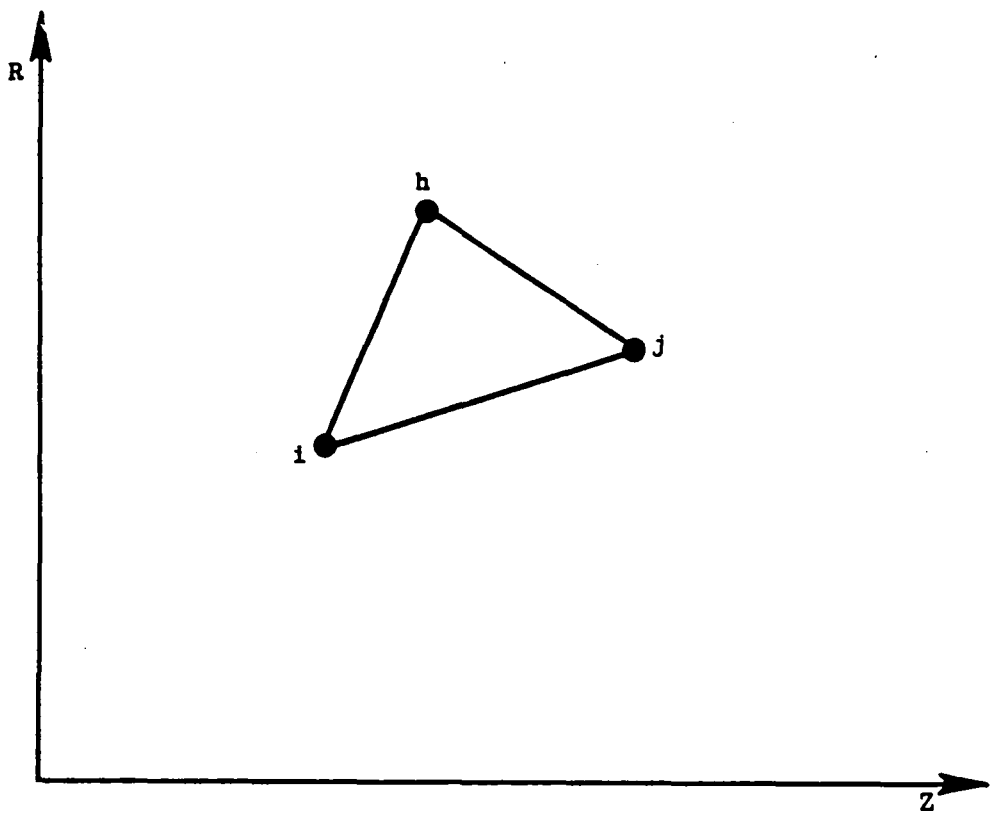

Figure 1. Finite Element Node Ordering.

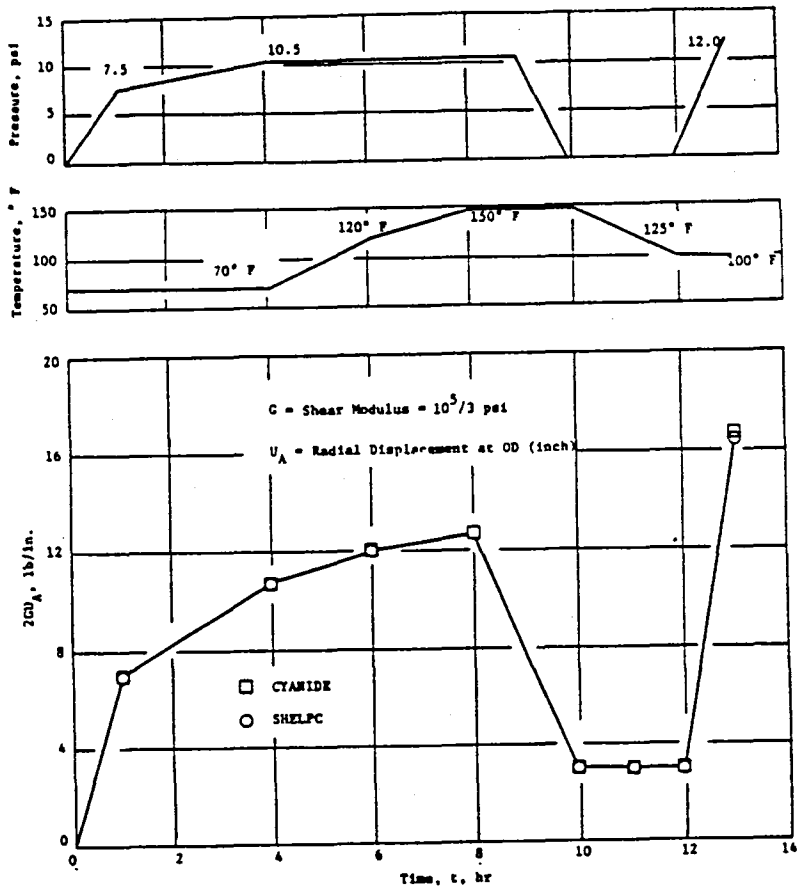

Figure 2. Load, Temperature History; Elastic-Plastic Displacement Response of a Thick-Walled Cylinder.

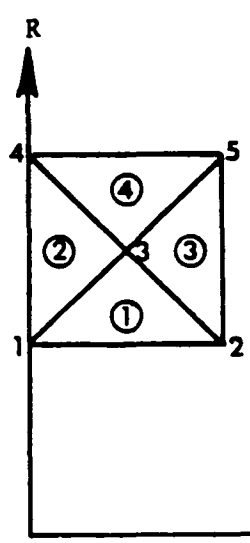

$E = 30 \times 10^6$ psi

$\nu = 0.3$

$\alpha = 6.0 \times 10^{-6}$ in/(in - ° F)

Node No.	R_i	Z_i
1	1.0	0.0
2	1.0	1.0
3	1.5	0.5
4	2.0	0.0
5	2.0	1.0

Figure 3. Thick-Walled Cyclinder Model Used for Combined Harmonic Loading Verification.

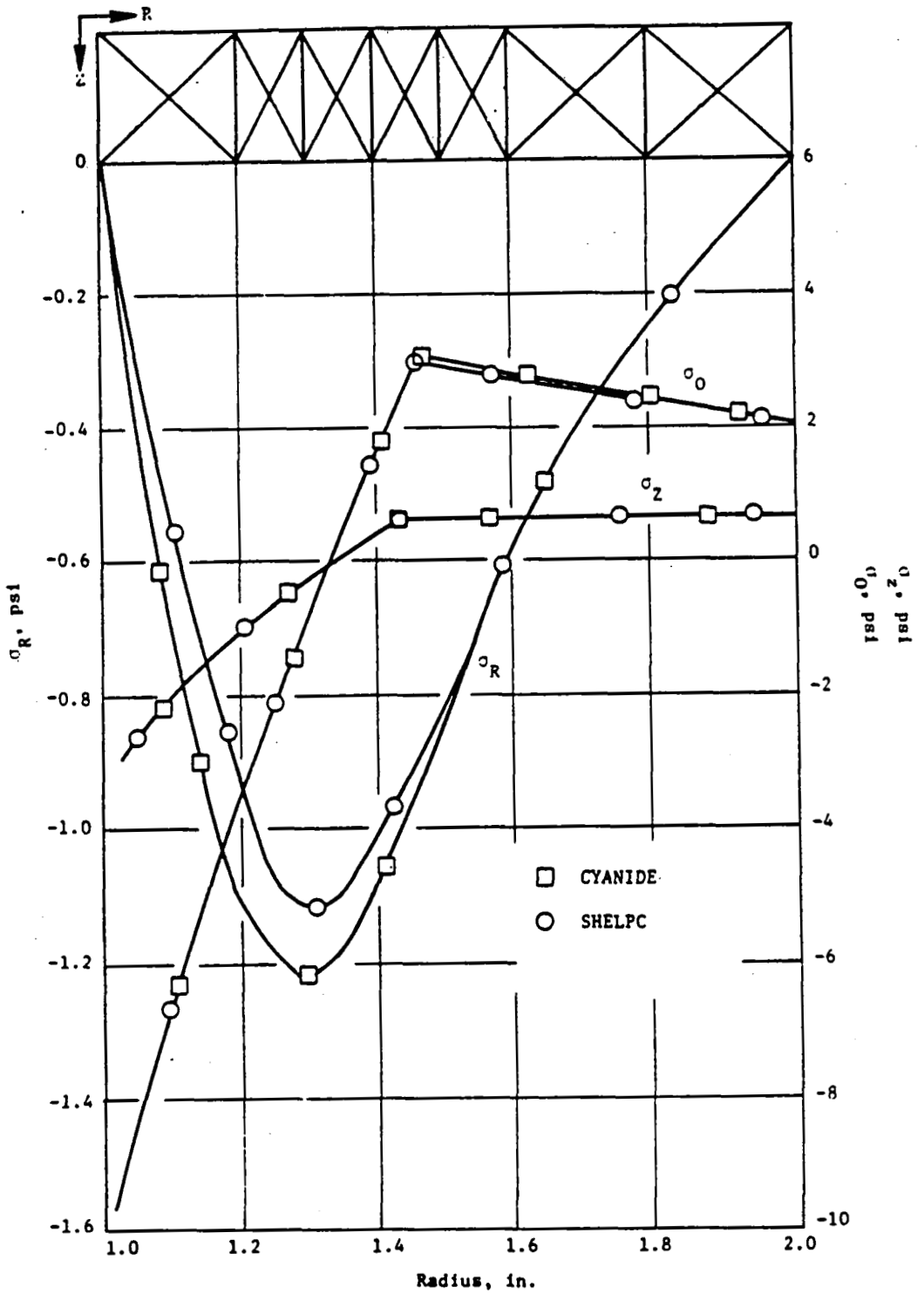

Figure 4. Residual Stress Distribution at Time = 10 hrs.

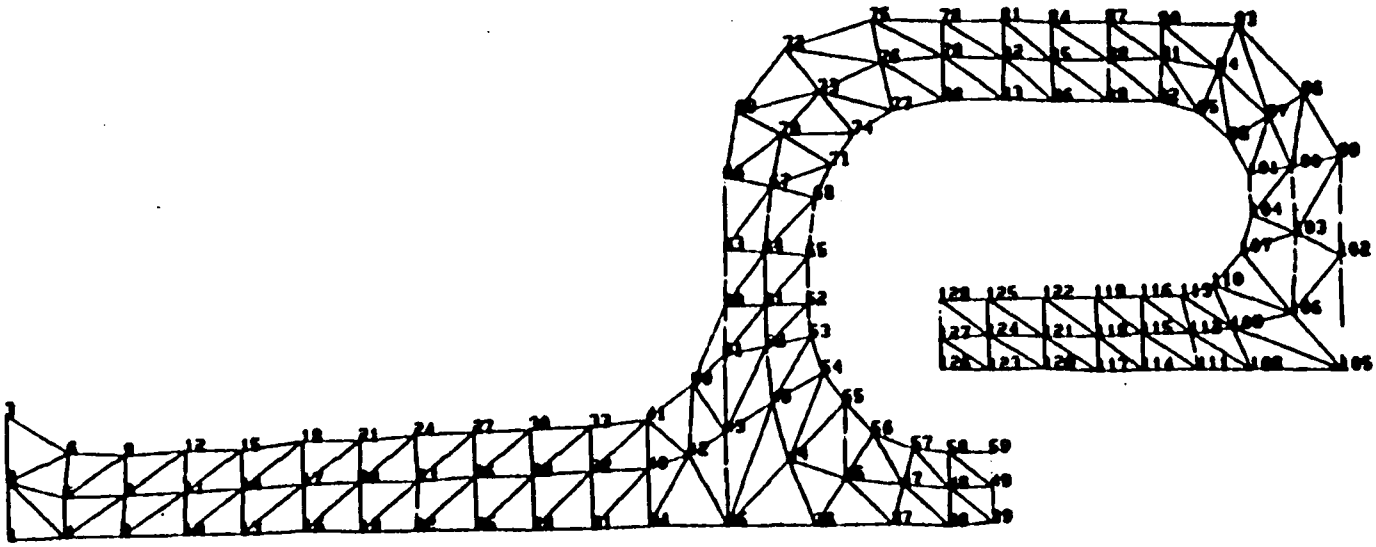

Figure 5. SHELPC Model for Combustor Lip.

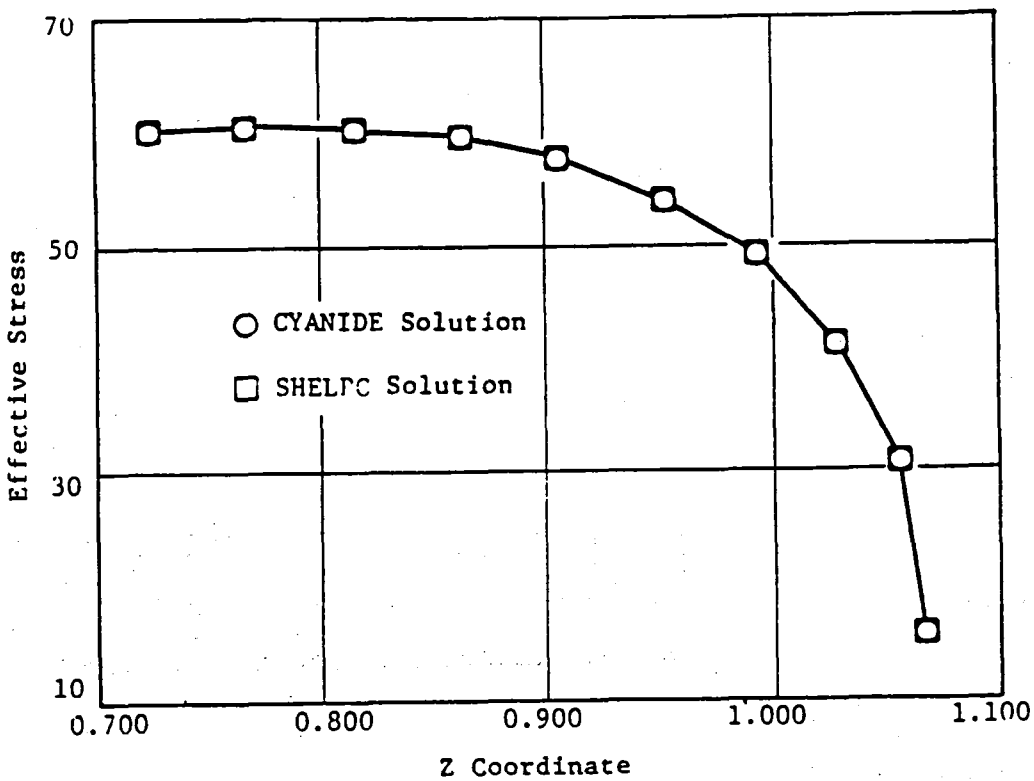

Figure 6. Effective Stress Comparison for Combustor Model.

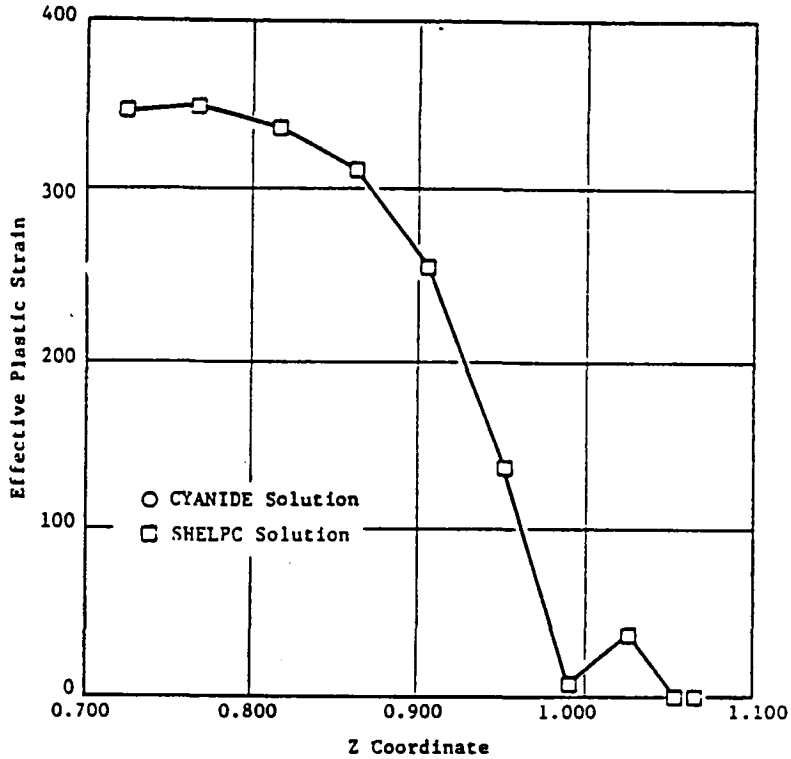

Figure 7. Effective Plastic Strain Comparison for Combustor Model.

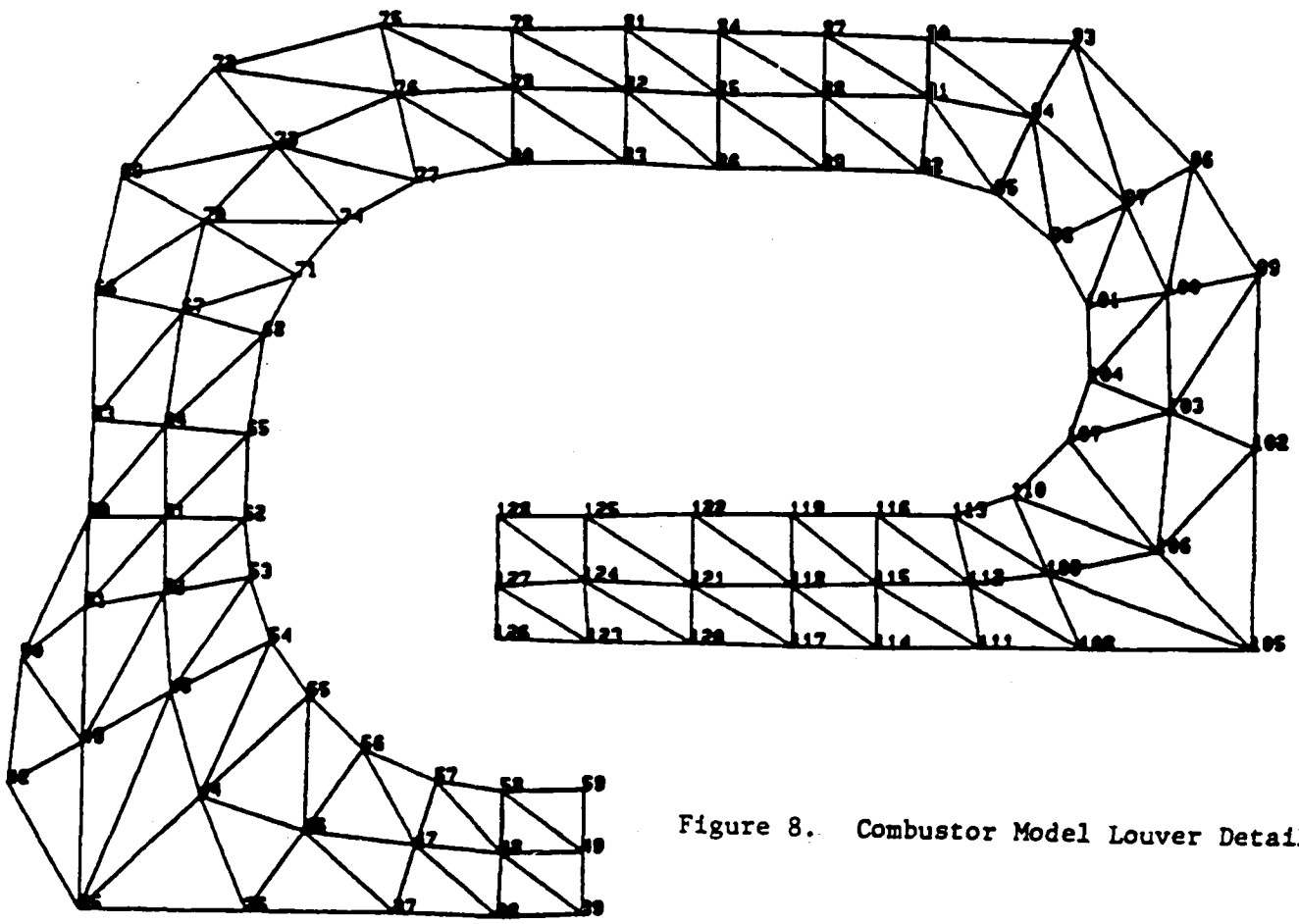

Figure 8. Combustor Model Louver Detail.

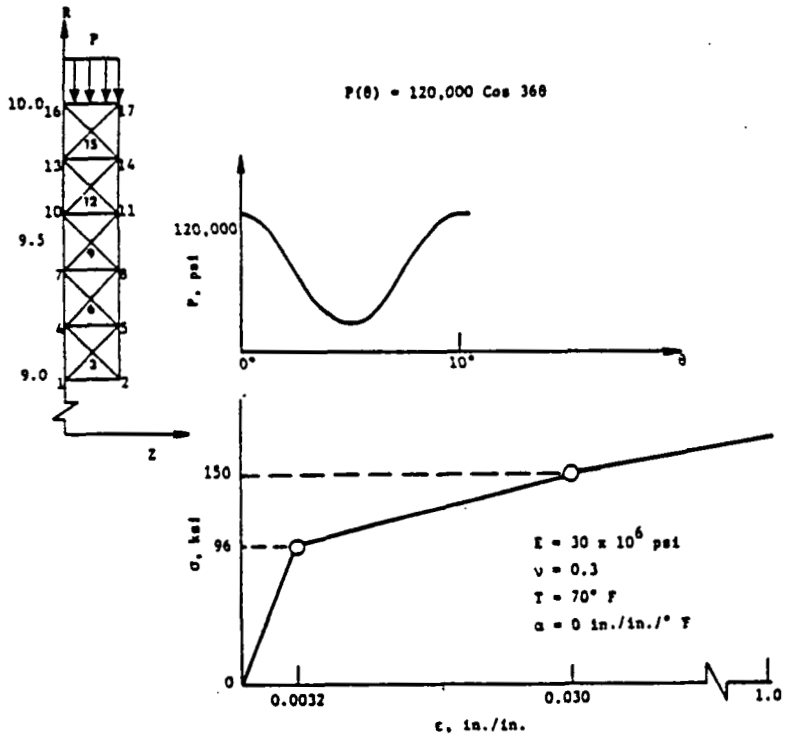

Figure 9. Ring Under Harmonic Pressure Load at OD.

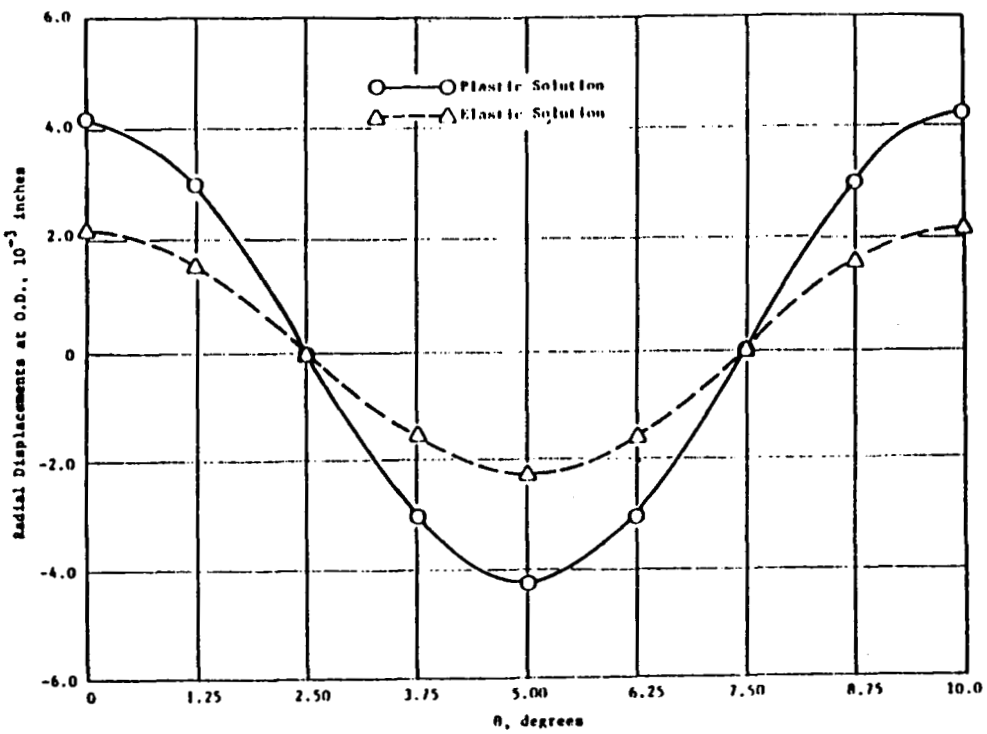

Figure 10. SHELPC Predictions of Radial Displacements.

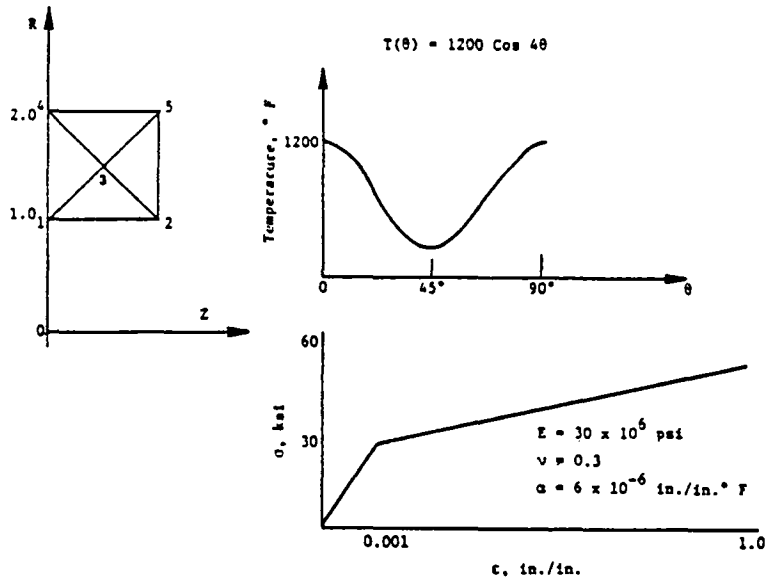

Figure 11. Cylinder Under Harmonic Thermal Load.

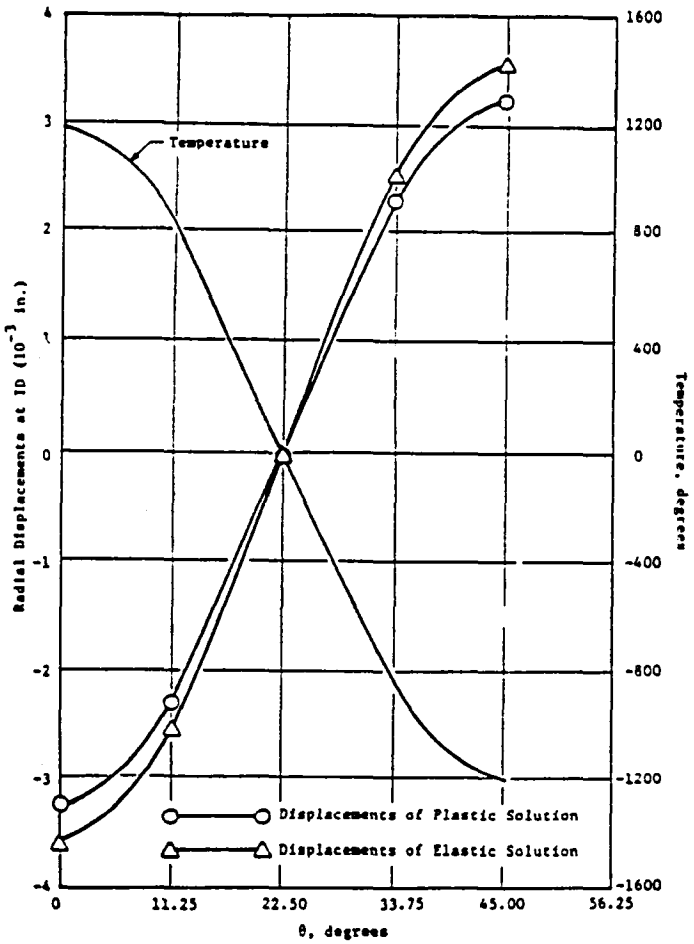

Figure 12. SHELPC Predictions for Hot Streak.